RF Energy Harvesting in Minimization of Age of Information with Updating Erasures

Fariborz Lohrabi Pour[1], Harrison Williams[2], Matthew Hicks[2], and Dong Sam Ha[1]
[1]*Multifunctional Integrated Circuits and System (MICS) Group*
[1]*Bradley Department of Electrical and Computer Engineering*
[2]*Department of Computer Science*
[1,2]Virginia Tech, Blacksburg, Virginia, 24061, USA
E-mail: {fariborzlp, hrwill, mdhicks2, ha} @vt.edu

***Abstract*—This paper presents an investigation into practical considerations in minimization of Age of Information (AoI) for the system architectures with and without updating feedback. To study the impact of the critical characteristics of the energy harvesters on the computing accuracy of the average AoI, an RF energy harvester with a half-wavelength patch antenna array along with a 3-stage voltage rectifier is designed and prototyped with the center frequency of 2.655 GHz. A cryptography algorithm is also implemented on a μ-controller unit to imitate the behavior of a practical processing unit. The paper shows measurement results and discusses the impact of the non-idealities in the energy harvester on the average AoI of the system. It also shows that the nonlinear power conversion profile of the energy harvester can increase the average AoI to over 300% compared to an ideal and linear energy harvester.**

***Index Terms*—AoI, Cryptography, Energy harvester, Internet of Things (IoT), PCE, Transmitter.**

I. Introduction

Low-power and low-data-rate Internet-of-Things (IoT) devices become increasingly pervasive in commercial, industrial, and consumer settings [1]; emerging network standards are prepared to support up to one million IoT-type devices per square kilometer [2]. Massive deployment scales and the resulting need for self-sustainable, maintenance-free sense/compute/transmit platforms have inspired system architectures that are powered from ambient RF sources (e.g., WiFi and 5G signals) rather than batteries. However, the power conversion efficiency (PCE) of the energy harvesters and their capacity to store energy is limited, which indicates the necessity of adopting optimal energy management policies to maximize the *"freshness"* of the transmitted information in status update systems.

The realm of age of information (AoI) has been introduced as a performance metric to quantify the freshness of data at the receiver [3]. The concept of AoI mostly focuses on energy-limited devices, such as IoT tags and sensors, which can be powered by an energy harvester as a sustainable energy resource for transmissions [4]. Several works have introduced optimal status updating policies to minimize AoI in such systems with different properties [3]–[7]. They mostly model the energy harvesting circuit with a fixed transfer function independent of the amount of power received by the energy harvester. Also, the power dissipated by the transmitter to transmit a single information packet is assumed as a normalized energy unit. However, the performance of the energy harvester is strongly dependent on the amount of received power, antenna efficiency, and the power converter. Further, the propagation delay of the energy harvester along with its load impedance can significantly impact the operating condition of the transmitter and hence, the optimum updating policy. Therefore, although the proposed policies might minimize AoI, ignoring such operating dependencies might cause sub-optimal operating condition in practical applications.

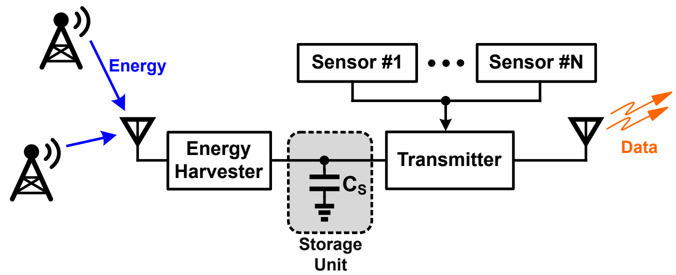

Fig. 1: Block diagram of a typical self-sustainable IoT tag.

Fig. 1 shows a typical self-sustainable IoT device. The RF signals traveling through the environment are received by the antenna and converted to DC power to be stored for the transmitter. The stored energy will then be consumed by the transmitter to transmit the sensed information to a receiver or gateway, based on the designated status updating policy. In this paper, we design and prototype a test bench to investigate the impact of crucial characteristics of the energy harvester and the transmitter on the average AoI with updating erasures. Our investigation includes the system model with and without status updating feedback since the optimal updating policy of these architectures is different [7].

This paper is organized as follows. Section II presents the design procedure of a typical self-sustainable IoT device along with the system model and optimal status updating policy. Section III discusses the experimental results. Finally, Section IV concludes the paper.

II. Design of a Self-Sustainable IoT Device

In this section, we present the design procedure of a practical IoT device, including an energy harvester and a

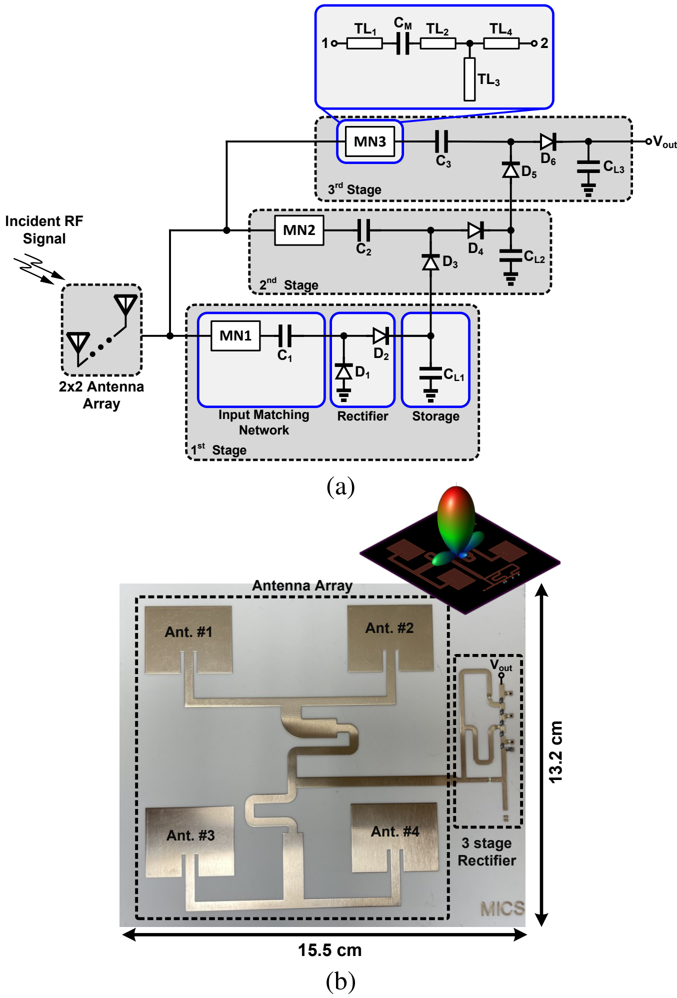

Fig. 2: (a) Schematic, and (b) photograph of the prototyped RF energy harvester.

processor. We also present a system model to study the impact of the characteristics of the energy harvester on the AoI of the receiver.

A. RF Energy Harvesting

The availability of RF signals in different environments is a result of wireless communications such as cellular networks, WiFi, Bluetooth, and long-range communication [8]. Therefore, these RF signals can be considered as an energy source to provide power for low-power devices (e.g. IoT tags) [9]. The schematic of the introduced RF energy harvester is shown in Fig. 2 (a). A 2×2 half-wavelength patch antenna array is designed at the center frequency of 2.655 GHz with 70 MHz spanning around the center frequency. This enables the energy harvester to receive RF signals from LTE-M, LTE NB-IoT, and 5G NB-IoT sources with relatively high directivity. The antenna is prototyped on a piece of Rogers 4003C substrate with a measured peak gain of 11.7 dB at 2.63 GHz.

A three-stage half-wave voltage doubler is also designed utilizing Skyworks SMS7620 low on-resistance and low forward voltage diodes to convert the received RF signal to a DC voltage across the output capacitor (C_{L_3}). This configuration is able to provide higher output voltage by ≈ 3 times compared to a single-stage voltage doubler, resulting in longer operation time for the transmitter to be discussed in Section III [10]. Fig. 3 shows the power conversion efficiency of the rectifier obtained as follows.

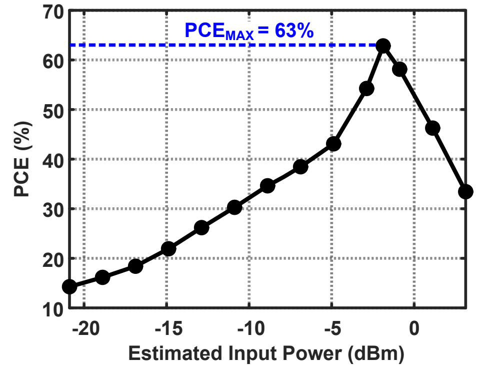

Fig. 3: Measured unloaded PCE of the rectifier.

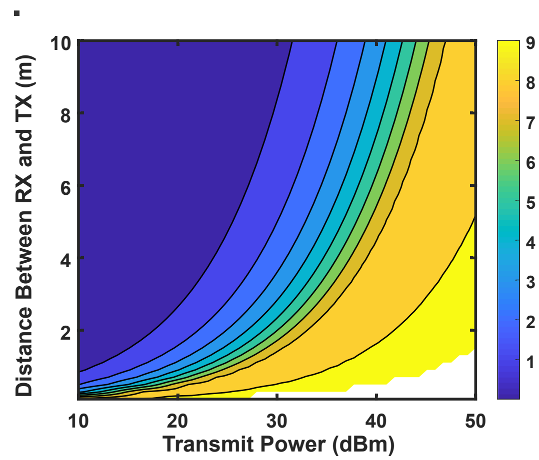

Fig. 4: Measured unloaded output voltage of the rectifier versus transmitted power and distance between the transmitting antenna and the rectenna.

$$PCE(\%) = \frac{Output\ DC\ Power}{Received\ RF\ Power} \times 100 \qquad (1)$$

The maximum PCE of the rectifier is measured to be 63% at an input power of ≈ 3 dBm. It can be seen that the PCE profile of the rectenna is a function of the input power to the rectifier. Modeling the received energy with only a one-dimensional Poisson function does not reflect the realistic characteristics of the energy harvester. Therefore, the input power needs to be considered when computing the AoI.

Fig. 4 shows the measured output voltage of the rectifier. The line-of-sight (LOS) distance between the rectenna (RX) and transmitter (TX) was swept while the transmitted power varied from 10 to 50 dBm. It can be seen that a maximum output voltage of ≈ 9 V is achieved across the output capacitor $C_{L_3} = 2200\ \mu$F.

B. Processing Unit

The energy harvesting circuit drives a commercial low-power μ-controller unit (MCU) MSP430FR5994 [11], suitable

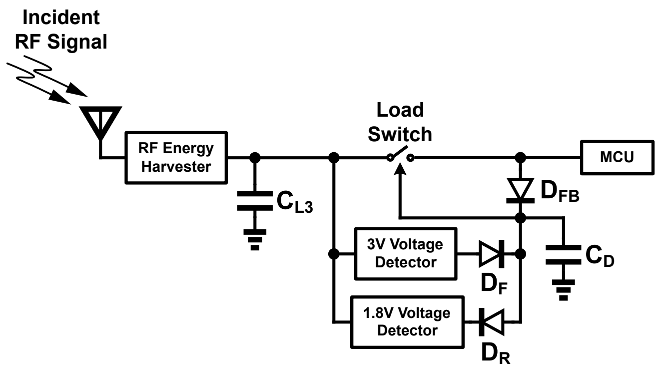

Fig. 5: Load switch circuit controlling the MCU current drawn from the energy harvester.

for batteryless systems operating between 1.8 - 3.6 V with an active current draw of 192 μA at the 1 MHz clock frequency. Fig. 5 shows the structure of the full energy harvesting system. The energy harvester charges C_{L_3} to a trigger operational voltage of 3 V. The voltage detector also enables the load switch, connecting the MCU to the capacitor and energy harvester. The buffer capacitor ensures a minimum operating time for software on the MCU, even if power input from the harvesting circuit ceases. After enabling at 3 V, the MCU runs until the buffer capacitor reaches the minimum 1.8 V. Between 3 V and 1.8 V, the feedback from the load switch output keeps the switch conducting. Once the input voltage falls below 1.8 V, the 1.8 V detector pulls the enable voltage for the load switch down, disconnecting the MCU and allowing the harvesting circuit to recharge the capacitor. While active, the MCU continuously performs AES128 encryptions in software.

Depending on the ambient power conditions, the MCU may periodically lose power if its current draw is greater than what the harvester can supply or if the input power is suddenly cut off. Software sustains execution across these power cycles using previously developed techniques for intermittent computing to make forward progress despite losing power [12]–[14]. The MCU periodically saves snapshots of the program state in non-volatile, on-chip ferroelectric RAM. Upon reset, the software restarts execution from these state snapshots rather than re-executing from the beginning.

C. System Model and Optimal Status Updating Policy

In this work, we use the system model introduced in [7]. The updating channel between the transmitter (source) and receiver is assumed imperfect; therefore, updating erasures can happen. Further, we investigate the impact of the energy harvester non-idealities on the system with and without updating feedback, where the transmitter receives instantaneous feedback or has no knowledge of update status.

It has shown in [7], that Best-effort Uniform updating with Retransmission (BUR) and Best-effort Uniform updating (BU) are optimal online policies for the system with and without feedback, respectively. It should be noted that these results are valid for the energy harvester presented in section II-A since its maximum output voltage is sufficiently larger than the minimum required supply voltage of the MCU. Further, similar to the original work, we assume that the processing time of the MCU is negligible compared to the long-term average AoI. Defining the total amount of harvested energy S_n, as the Poisson arrival process in $[l_{n-1}, l_n)$, the energy level right before the update time can be expressed as

$$E(l_1^-) = E_0 + S_1, \tag{2a}$$
$$E(l_n^-) = E(l_{n-1}^-) + S_n - 1, \quad n = 2, 3, ... \tag{2b}$$

with

$$E(l_n^-) \geq E_T, \quad n = 2, 3, ... \tag{3}$$

where E_T is the energy required to transmit an update by the transmitter. By following the same methodology as described in [7], the lower bound for the long-term average AoI for a system without feedback can be calculated as

$$\min \; AoI_{woFB} = \frac{2-p}{2p} \tag{4}$$

where p is the probability of a successfully received update by the receiver. The lower bound for a system with perfect feedback can also be obtained as

$$\min \; AoI_{wFB} = \frac{1}{2p}. \tag{5}$$

It can be seen from (4) and (5) that the feedback reduces the long-term average AoI.

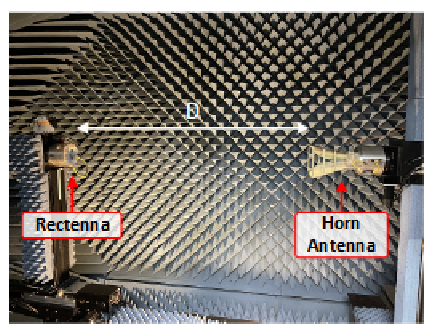

(a)

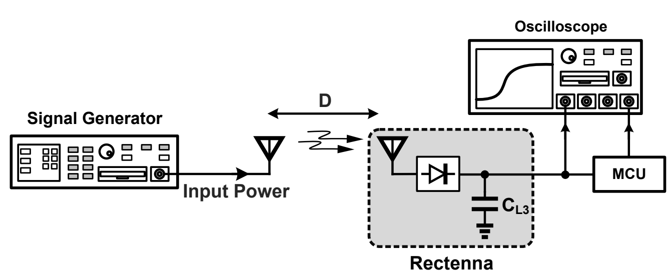

(b)

Fig. 6: (a) Photograph, and (b) block diagram of the measurement setup.

III. Experimental Results

Fig. 6 shows the measurement setup. A horn antenna is adopted as the transmitting antenna that is placed inside an anachronic chamber to minimize interference. The RF signal generator feeds the transmitting antenna with a variable power signal at random Poisson process times. The rectenna receives the transmitted power and converts it to DC voltage across C_{L_3}. The stored energy across the output will then be used to power the MCU. Further, the distance between the transmitter and receiver is fixed at 2 m.

To investigate the impact of the PCE profile of the energy harvester on the average AoI, the transmit power range is adjusted to receive the desired power range at the input of the rectifier. Fig. 7 shows the dependency of the normalized average AoI to the dynamic range of the received power. It can be seen that the AoI for both updating policies increases as the power range expands. The minimum AoI is achieved when the transmit power is fixed to achieve the maximum rectifier PCE. Refer to Fig. 3.

It is noted that although the minimum AoI should match the results in [7], but the measured result is slightly different from the original work. This can be attributed to the finite storage capacity of the energy harvester in the prototyped circuit. Therefore, by increasing the capacitance of C_{L_3} the results of this work would converge to the ones in [7]. Further, the system with feedback is more sensitive to the non-idealities of the energy harvester. It can also be noticed that the average AoI can increase by approximately 280%. One proper strategy to reduce the impact of the PCE profile on the AoI is to expand the flatness of the PCE curve using an adaptive bias voltage technique [15].

Moreover, the impact of the charging time constant ($\tau \propto C_{L_3}$) on the average AoI follows the same variation trend as the input power range. This is a valid conclusion as long as the random incidents that the rectenna receives power are similar to the experiment in Fig. 7. However, as it is shown in Fig. 8, the influence of the charging time constant on the average AoI can be more severe. This could pose a challenge to the design of the system, since increasing the time constant increases the stored energy while increasing the AoI.

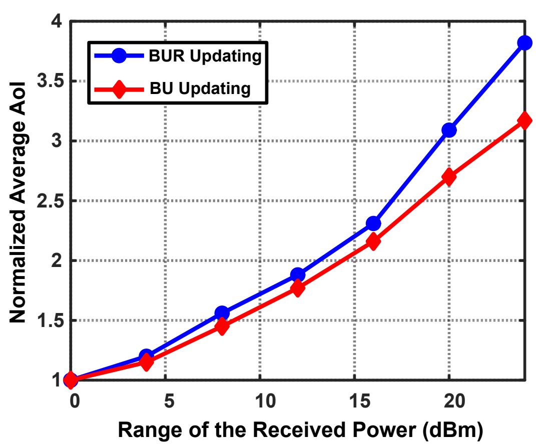

Fig. 7: Measured normalized average AoI versus the range of variable received power by the rectifier at 2.63 GHz.

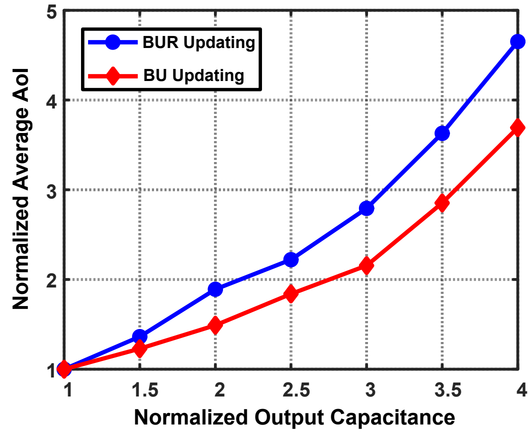

Fig. 8: Measured normalized average AoI versus the normalized output capacitance (i.e., $C_{L_3}/(1100\ \mu F)$) at 2.63 GHz.

IV. Conclusion

In this paper, we considered a system model with erasures and optimal online status update policies to investigate the impact of the non-idealities of the circuit design on the average AoI of the system. We also described the design of an energy harvester and a processing unit that was used to build a test bench to measure these effects and possible performance degradation. We showed that the non-constant energy harvester profile, along with the charging time constant of the energy harvester, can significantly increase the average AoI. Further, we briefly mentioned approaches to overcome the negative effect of the energy harvester non-idealities on the AoI.

Acknowledgment

This research was supported in part by the National Science Foundation Award no. 1814477. The project depicted is sponsored by the Defense Advanced Research Projects Agency. The content of this information does not necessarily reflect the position or the policy of the Government, and no official endorsement should be inferred. Approved for public release, distribution is unlimited.

REFERENCES

[1] T. Mai, H. Yao, S. Guo, and Y. Liu, "In-network computing powered mobile edge: Toward high performance industrial IoT," *IEEE Network*, vol. 35, no. 1, pp. 289–295, 2020.

[2] A. Dogra, R. K. Jha, and S. Jain, "A survey on beyond 5g network with the advent of 6g: Architecture and emerging technologies," *IEEE Access*, vol. 9, pp. 67 512–67 547, 2021.

[3] R. D. Yates, Y. Sun, D. R. Brown, S. K. Kaul, E. Modiano, and S. Ulukus, "Age of information: An introduction and survey," *IEEE Journal on Selected Areas in Communications*, vol. 39, no. 5, pp. 1183–1210, 2021.

[4] A. Arafa, J. Yang, and S. Ulukus, "Age-minimal online policies for energy harvesting sensors with random battery recharges," in *2018 IEEE International Conference on Communications (ICC)*, 2018, pp. 1–6.

[5] B. T. Bacinoglu, Y. Sun, E. Uysal, and V. Mutlu, "Optimal status updating with a finite-battery energy harvesting source," *Journal of Communications and Networks*, vol. 21, no. 3, pp. 280–294, 2019.

[6] S. Leng and A. Yener, "Age of information minimization for an energy harvesting cognitive radio," *IEEE Transactions on Cognitive Communications and Networking*, vol. 5, no. 2, pp. 427–439, 2019.

[7] S. Feng and J. Yang, "Age of information minimization for an energy harvesting source with updating erasures: Without and with feedback," *IEEE Transactions on Communications*, vol. 69, no. 8, pp. 5091–5105, 2021.

[8] M. A. Ullah, R. Keshavarz, M. Abolhasan, J. Lipman, K. P. Esselle, and N. Shariati, "A review on antenna technologies for ambient rf energy harvesting and wireless power transfer: Designs, challenges and applications," *IEEE Access*, vol. 10, pp. 17 231–17 267, 2022.

[9] R. Reed, F. L. Pour, and D. S. Ha, "An efficient 2.4 ghz differential rectenna for radio frequency energy harvesting," in *2020 IEEE 63rd International Midwest Symposium on Circuits and Systems (MWSCAS)*, 2020, pp. 208–212.

[10] Z. Zeng, S. Shen, X. Zhong, X. Li, C.-Y. Tsui, A. Bermak, R. Murch, and E. Sánchez-Sinencio, "Design of sub-gigahertz reconfigurable rf energy harvester from 22 to 4 dbm with 99.8% peak mppt power efficiency," *IEEE Journal of Solid-State Circuits*, vol. 54, no. 9, pp. 2601–2613, 2019.

[11] T. Instruments, "MSP430FR599x, MSP430FR596x Mixed-Signal Microcontrollers," January 2021, https://www.ti.com/lit/ds/symlink/msp430fr5994.pdf.

[12] B. Ransford, J. Sorber, and K. Fu, "Mementos: System Support for Long-Running Computation on RFID-Scale Devices," in *Architectural Support for Programming Languages and Operating Systems (ASPLOS)*, 2011.

[13] J. V. D. Woude and M. Hicks, "Intermittent computation without hardware support or programmer intervention," in *USENIX Symposium on Operating Systems Design and Implementation*, ser. OSDI, Nov. 2016, pp. 17–32.

[14] K. Maeng, A. Colin, and B. Lucia, "Alpaca: Intermittent execution without checkpoints," in *International Conference on Object-Oriented Programming, Systems, Languages, and Applications*, ser. OOPSLA, Oct. 2017, pp. 96:1–96:30.

[15] Z. Hameed and K. Moez, "A 3.2 v –15 dbm adaptive threshold-voltage compensated rf energy harvester in 130 nm cmos," *IEEE Transactions on Circuits and Systems I: Regular Papers*, vol. 62, no. 4, pp. 948–956, 2015.